UC Irvine
UC Irvine Previously Published Works

Title
Biophysical stimulation induces demyelination via an integrin-dependent mechanism

Permalink
https://escholarship.org/uc/item/7cm8j7td

Journal
Annals of Neurology, 72(1)

ISSN
0364-5134

Authors
Lin, Michael Y
Frieboes, Laura S
Forootan, Maryam
et al.

Publication Date
2012-07-01

DOI
10.1002/ana.23592

Copyright Information
This work is made available under the terms of a Creative Commons Attribution License, availalbe at https://creativecommons.org/licenses/by/4.0/

Peer reviewed

eScholarship.org Powered by the California Digital Library
University of California

Biophysical Stimulation Induces Demyelination via an Integrin-Dependent Mechanism

Michael Y. Lin, MD, PhD,[1] Laura S. Frieboes, PhD,[2] Maryam Forootan, BS,[1] Winnie A. Palispis, BS,[1] Tahseen Mozaffar, MD,[3] Matiar Jafari, BS,[4] Oswald Steward, PhD,[4,5] Christine M. Gall, PhD,[4,5] and Ranjan Gupta, MD[1,2,4]

Objective: Chronic nerve compression (CNC) injuries occur when peripheral nerves are subjected to sustained mechanical forces, with increasing evidence implicating Schwann cells as key mediators. Integrins, a family of transmembrane adhesion molecules that are capable of intracellular signaling, have been implicated in a variety of biological processes such as myelination and nerve regeneration. In this study, we seek to define the physical stimuli mediating demyelination and to determine whether integrin plays a role in the demyelinating response.
Methods: We used a previously described in vitro model of CNC injury where myelinating neuron–Schwann cell cocultures were subjected to independent manipulations of hydrostatic pressure, hypoxia, and glucose deprivation in a custom bioreactor. We assessed whether demyelination increased in response to applied manipulation and determined whether integrin-associated signaling cascades are upregulated.
Results: Biophysical stimulation of neural tissue induced demyelination and Schwann cell proliferation without neuronal or glial cytotoxicity or apoptosis. Although glucose deprivation and hypoxia independently had minor effects on myelin stability, together they potentiated the demyelinating effects of hydrostatic compression, and in combination, significantly destabilized myelin. Biophysical stimuli transiently increased phosphorylation of the integrin-associated tyrosine kinase Src within Schwann cells. Silencing this integrin signaling cascade blocked Src activation and prevented pressure-induced demyelination. Colocalization analysis indicated that Src is localized within Schwann cells.
Interpretation: These results indicate that myelin is sensitive to CNC injury and support the novel concept that myelinating cocultures respond directly to mechanical loading via activating an integrin signaling cascade.
ANN NEUROL 2012;72:112–123

Chronic nerve compression (CNC) injuries such as carpal tunnel syndrome, cubital tunnel syndrome, and spinal nerve root stenosis occur at fibro-osseous nerve tunnels where direct abutment against rigid structures leads to sustained mechanical insults, causing pain, paresthesia, and paralysis. Traditionally, research on CNC injury has focused on the secondary effects of compression on peripheral nerve microanatomy. Examples include disruption of neuronal microcirculation,[1,2] induction of intracellular hydrostatic pressure gradients,[3] and alteration of cellular substructures.[2]

Recent evidence indicates that cells can directly respond to physiological mechanical loading,[4–8] suggesting the existence of a molecular sensor capable of translating mechanical stresses into cellular responses. One particularly attractive candidate for mechanotransduction is the integrin family of heterodimeric transmembrane proteins that bind the extracellular matrix[9,10] and are capable of intracellular signal transduction.[11–13]

Here we developed a custom bioreactor, where purified myelinating Schwann cell (SC)–dorsal root ganglion cocultures can be subjected to stimuli known to be associated with CNC injury. Candidate stimuli include oxygen tension, glucose deprivation, and hydrostatic pressure that we collectively termed *biophysical stimuli*. This in vitro injury model allows the determination of the effects of these stimuli on cellular behavior, and enabled

View this article online at wileyonlinelibrary.com. DOI: 10.1002/ana.23592

Received Jan 8, 2012, and in revised form Feb 19, 2012. Accepted for publication Mar 15, 2012.

Address correspondence to Dr Gupta, Department of Orthopedic Surgery, 2216 Gillespie Neuroscience Research Facility, Irvine, CA 92697-4292. E-mail: ranjang@uci.edu

From the [1]Department of Orthopedic Surgery, [2]Department of Biomedical Engineering, [3]Department of Neurology, [4]Department of Anatomy and Neurobiology and [5]Department of Neurobiology and Behavior, University of California, Irvine, CA.

 © 2012 American Neurological Association

the identification of the reactive cell and the molecular signals mediating the cellular response.

Materials and Methods

Dorsal Root Ganglion Neuron and SC Cocultures

Dorsal root ganglia (DRGs) were dissected from embryonic day 14 Sprague Dawley (SD) rats and purified according to established techniques.[14] Briefly, collected DRGs were digested with 0.05% trypsin, then triturated and centrifuged. The cells were seeded at approximately 25×10^4 cells onto 1cm Thermonox coverslips (Nalge Nunc, Rochester, NY) coated with Rat collagen (30ng/ml; Sigma, St Louis, MO). Cells were maintained in warm culture medium consisting of glucose-free Neurobasal Medium (Millipore, Billerica, MA), supplemented with insulin-free B27 (2%, Millipore), glucose (20mM), L-glutamine (0.5mM, Millipore), nerve growth factor 2.5S (10ng/ml), and penicillin/streptomycin sulfate (1:50). Contaminating non-neuronal cells were eliminated with 3 cycles of culture medium supplemented with 10μM 5′-fluoro-2′deoxyuridine and 10μM uridine (Sigma). To establish the cocultures, purified SCs (see below) were seeded onto purified DRG neurons at a density of 2×10^5 cells per dish. The resulting cocultures were initially maintained in serum-free medium for about 1 week. Fifty micrograms per milliliter L-ascorbic acid and 10% fetal bovine serum were subsequently added to induce myelination (Fig 1A).

SCs were extracted from sciatic nerves of 3-day-old SD neonatal rats and purified using the modified Brockes technique.[15] Cultures were plated on poly-D-lysine-coated Petri dishes (BD Biosciences, San Jose, CA) and expanded in supplemented Dulbecco modified Eagle/F12 media (Millipore).

Bioreactor

The previously described bioreactor[16] was pressurized with a diaphragm pump while a small, regulated amount of air was allowed to escape (0.5 standard cubic feet per hour) to maintain continual gas exchange. Sensors were used to monitor internal pressure, pH, and dissolved oxygen. A negative feedback control system regulated the flow of nitrogen and oxygen into the incubator, maintaining constant dissolved oxygen in the media during pressurization. Cells were exposed to biophysical stimuli for 24 hours, and then maintained at normal culture conditions (37°C, 5% CO2, 20% O2, 0mmHg) for 24 hours prior to assessment of demyelination. This period of delay ensures that all demyelinating response proceeds to completion, thus avoiding the possibility of underestimating demyelination. We applied 21mmHg of hydrostatic pressure in compression studies. Unless specified, experiments were performed in normal culture medium containing a total of 20mM glucose in atmospheric oxygen (~18%). Hypoxia studies were performed at 5% oxygen, and glucose deprivation was achieved by reducing the glucose media concentration to a total of 0.5mM or 5.0mM.

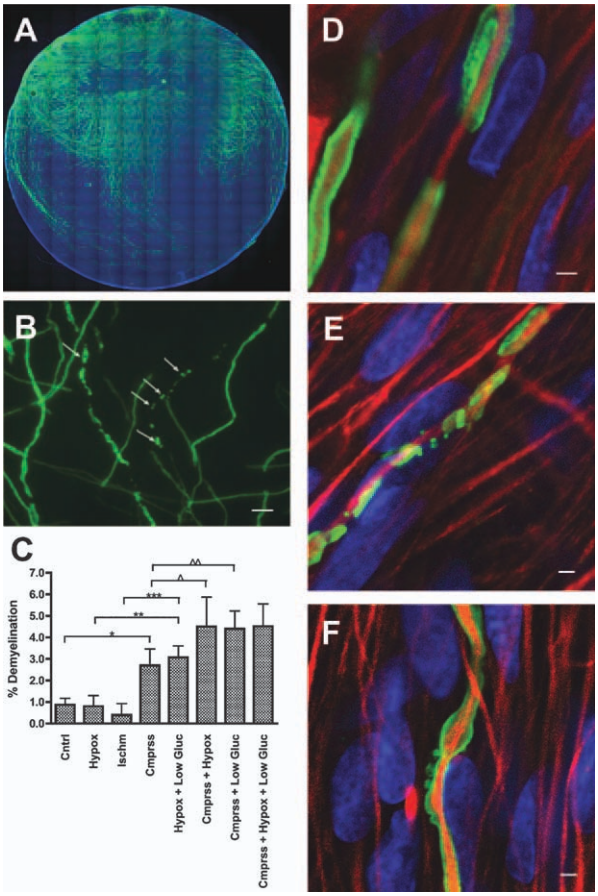

FIGURE 1: Biophysical stimuli induced demyelination in myelinating neuron–Schwann cell cocultures. Established myelinating cocultures were subjected to 24 hours of indicated biophysical stimuli in the custom bioreactor and subsequently immunostained for myelin basic protein. (A) A composite image of 144 sampling fields shows the typical myelination pattern of cocultures; scale bar = 1mm. (B) Twenty-four hours of hydrostatic compression and hypoxia produced demyelination, which is visible as fragmented myelin basic protein-positive myelin segments or myelin ovoids (*arrows*); scale bar = 50μm. Demyelination was assessed visually using an unbiased random stereology method as described by Larsen,[17] and summarized in the plot. (C) Biophysical Stimuli induces demyelination. Hypoxia (Hypox) or Glucose deprivation alone (Low Gluc) (2nd and 3rd bars from left) has negligible effect. Hydrostatic compression alone (Cmprss) produced statistically significantly more demyelination (4th bar from left, *t* test: **p* = 0.036, 1-tailed). Hypoxia combined with glucose deprivation also produced more demyelination than each stimulus alone (5th bar from left, ***p* = 0.0076, ****p* = 0.0045, 1-tailed). Hypoxia and glucose deprivation both potentiated the effect of compression, leading to more demyelination compared to compression alone (6th and 7th bars from left, ^*p* = 0.0348, ^^*p* = 0.0049, 1-tailed). Further combinations of biophysical stimuli produced only incrementally more demyelination (right-most bar). Cntrl = control.

Quantifying Labeled Cells

Labeled cells were viewed and photographed under epifluorescence on an Olympus (Tokyo, Japan) IX71 microscope. Using Visiopharm (Hørsholm, Denmark) imaging software, we used Stereology method to obtain a uniformly random and unbiased

estimate of the total number of labeled cells per coverslip.[17] In each case, a percentage is calculated via dividing the total number of affected cell (estimated via Stereological technique) by the total number of cells (also estimated via Stereological technique). In the case of demyelination, the percentage is calculated by dividing the estimated number of axons with fragmented myelin by the estimated total number of myelinating axons. To eliminate interobserver variations, the same investigator, blinded to the experimental groups, performed all the quantification analysis.

Myelin and Neurofilament Visualization

Myelination was visualized by immunolabeling DRG neuron/SC cocultures for myelin basic protein (MBP) or myelin-associated glycoprotein (MAG). Cells were fixed with 4% paraformaldehyde and cold methanol. Cell permeabilization and antigen revelation was achieved with the addition of Triton and incubation in pH 10 buffer. Nonspecific staining was blocked with 4% goat serum followed by overnight incubation in appropriate primary antibody (mouse anti-MBP antibody, 1:500 dilution, SMI-94R from Covance, Princeton, NJ; rabbit anti-MBP antibody from Millipore, 1:500 dilution; rabbit anti-MAG antibody from Santa Cruz Biotechnology, Santa Cruz, CA, 1:500 dilution; pan neurofilament antibody, 1:500 dilution, SMI-312 from Covance). Immunoreactivity was detected by incubating with fluorescently conjugated secondary immunoglobulin G (IgG) antibodies for 1 hour (fluorescein-conjugated IgG from Chemicon, Temecula, CA, 1:100 dilution; Alexa-conjugated IgG from Molecular Probes, Eugene, OR, 1:500 dilution).

Electron Microscopy

Cocultures were fixed in 2% paraformaldehyde and 2% glutaraldehyde and subsequently postfixed with 1% osmium tetroxide. Fixed specimen were dehydrated by sequential incubation in solutions of increasing ethanol concentration, and embedded in Embed 812 (Electron Microscopy Sciences, Hatfield, PA). Specimens were then polymerized overnight at 60°C and sectioned at 60nm using Leica Ultracut UCT ultramicrotome (Leica Microsystems, Bannockburn, IL). Ultrathin sections were mounted on copper grids, stained with uranyl acetate and lead citrate, and viewed using a JEOL 1400 transmission electron microscope (Jeol, Peabody, MA). Images were captured using a Gatan Orius camera (Gatan, Pleasanton, CA).

Assessment of Proliferation, Cytotoxicity, and Apoptosis

SC proliferation was evaluated by nuclear incorporation of 5′-bromo-2′-deoxy-uridine (BrdU), which was detected using a commercially available BrdU detection kit (Roche Applied Science, Indianapolis, IN). To access cytotoxicity, culture media was assayed for lactate dehydrogenase (LDH) using a Cytotoxicity Cell Death Detection kit (Roche Applied Science) according to the manufacturer's specifications. To analyze apoptosis, cocultures were double-labeled for neuron- or SC-specific markers (NeuN and S100, respectively) and terminal deoxynucleotidyl transferase dUTP nick end labeling (TUNEL) with an In Situ Cell Death Detection Kit per the manufacturer's instructions (Roche Applied Science).

Western Blotting

Lysate protein concentration was determined using a commercially available BCA Protein Assay kit (Thermo Scientific, Rockford, IL). Seventy-five to 100μg of protein was separated by 10% sodium dodecyl sulfate (SDS)-polyacrylamide gel electrophoresis, transferred to polyvinylidene difluoride membranes (0.2μm; BioRad, Hercules, CA), blocked with 5% dry skimmed milk, and incubated overnight at 4°C with primary antibodies.

For detection, goat antirabbit secondary antibody conjugated with horseradish peroxidase (HRP; 1:10,000 dilution, AP132P from Chemicon) or donkey antimouse secondary antibody conjugated with HRP (1:10,000 dilution, AP192P from Chemicon) was used. Blot development utilized Immobilon Western Chemiluminescent HRP Substrate (Millipore). Films were digitized with a color scanner, and images were analyzed using Quantity One image analysis software (BioRad). Quantitative results from Western blots were obtained after normalization of the densitometric data obtained from each antibody with that of β-actin or glyceraldehyde-3-phosphate dehydrogenase (GAPDH) on the same blot.

Primary Antibodies

The following primary antibodies were used for Western blot analysis: rabbit anti-pSrc (Y418, 1:250–1:500 dilution, #44660G from Invitrogen, Carlsbad, CA), rabbit anti-pPyk2 (Y402, 1:250–1:500 dilution, #44-618G from Invitrogen), rabbit anti-pPaxillin (Y31; 1:500 dilution, ab32115 from Abcam), rabbit anti-pPaxillin (Y118, 1:300–1:500 dilution, #44-772G from Invitrogen), rabbit antiactin IgG (1:5,000–1:10,000 dilution, A5060 from Sigma-Aldrich, St Louis, MO); mouse anti-GAPDH (clone 6C5, 1:5,000–1:10,000 dilution, MAB374 from Millipore). Total Src was detected with rabbit anti-Src antibody (1:500–1:1,000 dilution, #44656G from Invitrogen).

For functional blockade of integrin signaling, the following neutralizing integrin antibodies were used: mouse anti-human integrin β4 IgG (20μg/ml, MAB2058Z from Millipore), hamster antirat integrin β1 IgG (20μg/ml, #555002 from BD Biosciences), hamster antimouse Integrin αv IgG (20μg/ml, #553241 from BD Biosciences).

Colocalization Analysis

Cocultures were triple immunostained for localization of phosphorylated Src (rabbit anti-pSrc, Y418, 1:500 dilution, 44-618G from Invitrogen), S100 (see above for details), and neurofilament protein (mouse pan antineurofilament from Millipore, 1:500 dilution). Confocal images were acquired on a Zeiss (Oberkochen, Germany) 780 microscope equipped with a Plan-Apo ×63 (1.4 numerical aperture) water immersion objective. Images were taken at the Nyquist rate, ensuring no undersampling. Images are 512 × 512 pixels with 0.13μm Z-plane intervals.

Colocalization was assessed for each image using the colocalization module of IMARIS 7.1.1 (Bitplane AG, Zurich, Switzerland; 64-bit version), which uses an iterative threshold calculator that allows an impartial calculation of the intensities

in each channel.[18] Mander coefficient was used to assess a proportion of each protein colocalized within the other. Each image was automatically thresholded in the Colocalization module, and then a new colocalized channel was created that provided a Mander coefficient for each protein.

Statistical Analysis

Student t tests were used for planned comparisons of experimental and control samples. In all cases, $p < 0.05$ was considered statistically significant. Results are reported as mean ± standard error of the mean.

Results

Biophysical Stimuli Induce Demyelination in Myelinated Cocultures

Initial experiments focused on determining whether hydrostatic compression induced demyelination in myelinated cocultures. As the magnitude of pressure exerted on cells in compressive neuropathy is unknown, we loaded the cocultures with a pressure near the range of normal intracarpal pressure previously shown to induce a biologic response without detectable injury (21mmHg).[16] For hypoxia studies, we employed 5% oxygen, an oxygen tension that is well established in models of anoxia. Glucose deprivation was achieved by lowering the glucose concentration of culture media from the normal growing concentration of 20mM to 0.5 or 5.0mM.

Demyelination is readily apparent as the characteristic fragmented MBP-positive myelin segments or myelin ovoids (see Fig 1B; see also high-resolution confocal images in Figs 2B and C). Quantification of demyelination indicated that 24 hours of hydrostatic compression produced a 3-fold increase in the percentage of demyelination (see Fig 1C; control, 0.87 ± 0.30%, n = 9; compression, 2.69 ± 0.77%, n = 8; t test, $p = 0.036$). In isolation, neither hypoxia nor glucose deprivation caused significantly more demyelination relative to controls, but hypoxia combined with glucose deprivation produced a significant increase in demyelination compared to either stimulus alone (see Fig 1C; hypoxia + low glucose, 3.07 ± 0.53%, n = 8; hypoxia, 0.80 ± 0.50%, n = 8; low glucose, 0.40 ± 0.53%, n = 6; t test, $p = 0.0076$ and 0.0045). Similarly, hypoxia potentiated the demyelinating effect of hydrostatic compression, increasing the percent demyelination by 1.7% compared to hydrostatic compression alone (compression + hypoxia, 4.50 ± 1.37%, n = 8; t test, $p < 0.0348$). Glucose deprivation also potentiated the demyelinating effect of hydrostatic compression, increasing percent demyelination by 1.7% compared to hydrostatic compression alone (compression + low glucose, 4.40 ± 0.83%, n = 8; t test, $p < 0.0049$). Interestingly, further combinations of biophysical stimuli did not produce more demyelination compared to hydrostatic compression with hypoxia or glucose deprivation, as the observed demyelination was 4.5% when all 3 biophysical stimuli were applied (compression + hypoxia + low glucose, 4.52 ± 1.03%, n = 16; t test, $p > 0.05$).

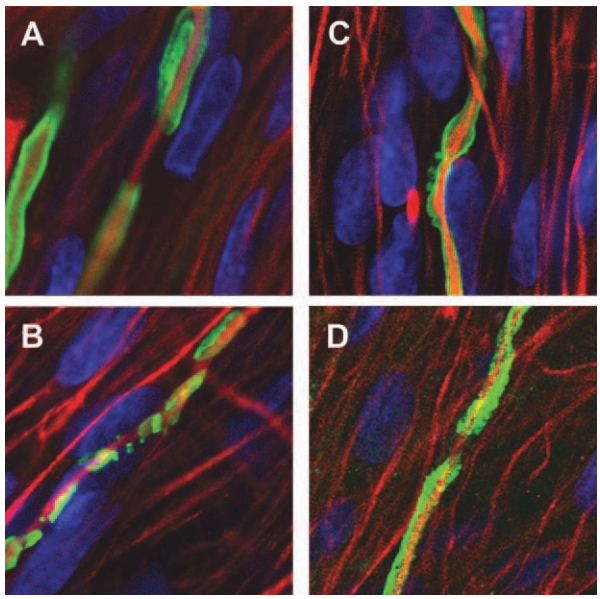

FIGURE 2: Demyelination occurred without axonal damage. To further characterize observed demyelination, control and stimulated samples were immunostained for myelin basic protein (MBP; green) and neurofilament (red) and subjected to high-power, high-resolution confocal microscopy. Representative images of normal (A), and demyelinated samples (B, C) are shown. In our culture system, demyelination occurs via fragmentation (B) and the formation of myelin ovoids (C). Myelin fragmentation and myelin ovoid formation (green) occurred without disruption of neurofilament continuity or morphology (red), indicating no axonal damage despite profound myelin disruption. To confirm the identity of stained myelin structures, a separate sample was immunostained for myelin-associated glycoprotein (MAG; green) and neurofilament (red; D). Although relatively punctate compared to MBP staining, the MAG-positive structure was identical in appearance compared to MBP-positive structures.

Biophysical Stimuli Do Not Induce Cell Damage in DRG Neuron/SC Cocultures

Demyelination is known to occur secondary to neuronal or SC death.[19,20] To ensure that this secondary demyelination did not confound our data interpretation, we first characterized the integrity of demyelinated axons with high-resolution confocal microscopy. Although biophysical stimulation induced fragmentation and myelin ovoids, it had no appreciable effect on axonal structure, as indicated by intact neurofilament immunostaining (red signals in Fig 2). We also performed MAG staining[21] of cocultures to confirm the identity of MBP-stained internodes. Although slightly punctate, MAG-

stained internodes are identical in appearance to those stained with MBP (compare Fig 2A vs 2D). These results confirm that myelin is readily identified with our immunohistochemical technique and that demyelination is reliably and unambiguously visualized.

We further assessed cell damage in our cultures via two other independent measures: cell membrane integrity assessed by LDH release and apoptosis activity indicated by TUNEL labeling. Investigated biophysical stimuli caused only a minor amount of LDH release compared with the control cultures (Fig 3A; control, 0.04 ± 0.51%; hypoxia, 0.92 ± 0.79%; compression, −0.19 ± 0.60%; n = 10 each). Combinations of biophysical stimuli induced paradoxically less LDH release compared to individual stimuli (see Fig 3A; hypoxia + low glucose, −0.16 ± 0.62%; compression + hypoxia, −2.44 ± 0.74%; compression + hypoxia + low glucose, −2.12 ± 0.80%; n = 10 each). These differences are, however, not statistically significant compared to controls or to the individual stimuli. Assessment of apoptosis via immunolabeling by TUNEL and in conjunction with cell-specific markers (S-100 for SCs, NeuN for neurons) indicated no significant increase in TUNEL-labeled SCs or neurons with 24 hours of hydrostatic compression (see Fig 3B; S100 control, 0.13 ± 0.097%, n = 8; S100 compression, 0.07 ± 0.033%, n = 12; NeuN control, 0.11 ± 0.074%, n = 13; NeuN compression, 0.16 ± 0.099%, n = 13).

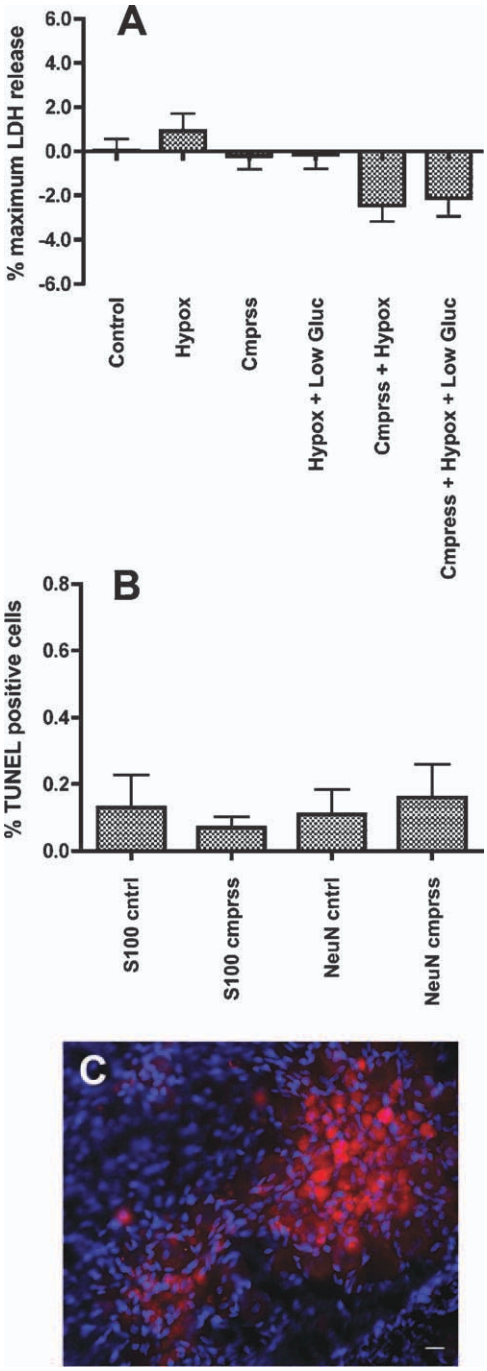

Ultrastructural Characterization of Biophysical Stimuli-Induced Demyelination

To further characterize demyelination induced by biophysical stimuli, we analyzed the myelin and axonal structures of control and stimulated cocultures at the

FIGURE 3: Biophysical stimuli are without cytotoxic or apoptotic effects on neuron–Schwann cell cocultures. Established cocultures subjected to indicated biophysical stimuli for 24 hours were analyzed for cytotoxicity via 2 independent methods; cell membrane integrity was assessed with released lactate dehydrogenase (LDH), and apoptosis activity was assessed by terminal deoxynucleotide transferase dUTP nick end labeling (TUNEL) assay. (A) Biophysical stimuli had negligible effect on cell membrane integrity. Released LDH was measured after 24 hours of exposure to biophysical stimuli. The released LDH was expressed as a percentage of maximal releasable LDH, which was obtained according to the following formula: % maximum LDH release = (experimental value − low control)/(high control − low control). The high control value was obtained by lysing cells using 2% Triton X-100, whereas the low control was the LDH present in normal cultures. Hypoxia (Hypox) or hydrostatic compression (Cmprss) individually produced negligible LDH release (2nd and 3rd bars from left). Combinations of biophysical stimuli produced paradoxically but statistically insignificantly less LDH in response to compression (4th, 5th, and 6th bars from left). (B) Biophysical stimuli produced negligible apoptosis activity. In a separate set of experiments, cocultures were compressed for 24 hours and subsequently double-stained for TUNEL and either Schwann cell marker S100 (left 2 bars) or neuronal marker NeuN (right 2 bars). In either case, there was negligible difference in TUNEL activity compared to control cultures, indicating no increased apoptosis in either Schwann cells or neurons. (C) A sample image of compressed coculture subsequently triple-labeled for TUNEL (green), neuronal marker NeuN (red), and Schwann cell nuclei (blue) is shown. There were no TUNEL-positive cells. Scale bar = 50μm. Gluc = glucose. [Color figure can be viewed in the online issue, which is available at www.annalsofneurology.org.]

ultrastructural level. As a positive control for demyelination, a set of coculture was exposed to dichloroacetate (DCA)[22] for comparison. Electron micrographs showed that myelinated cocultures formed compact myelin, which is seen ensheathed around axons. Careful examination of control cocultures showed that compact myelin is directly, uniformly, and continuously apposed around each axonal internode (Fig 4). With DCA treatment, there is characteristic demyelination along with axonal disruption that is visible at the ultrastructural level, with segmentation and unraveling of compact myelin as well as the formation of inclusion bodies and vacuoles within the compact myelin. Additionally, disrupted myelin is no longer closely apposed to axonal internodes. DCA-induced demyelination is clearly related to axonal injury, with the disruption of neurofilament architecture within the axonal internode. In contrast, samples exposed to the biophysical stimuli produced similar pattern of myelin disruption without detectable axonal pathology. This significant ultrastructural difference suggests that biophysical stimuli-induced demyelination occurs independent of axonal damage.

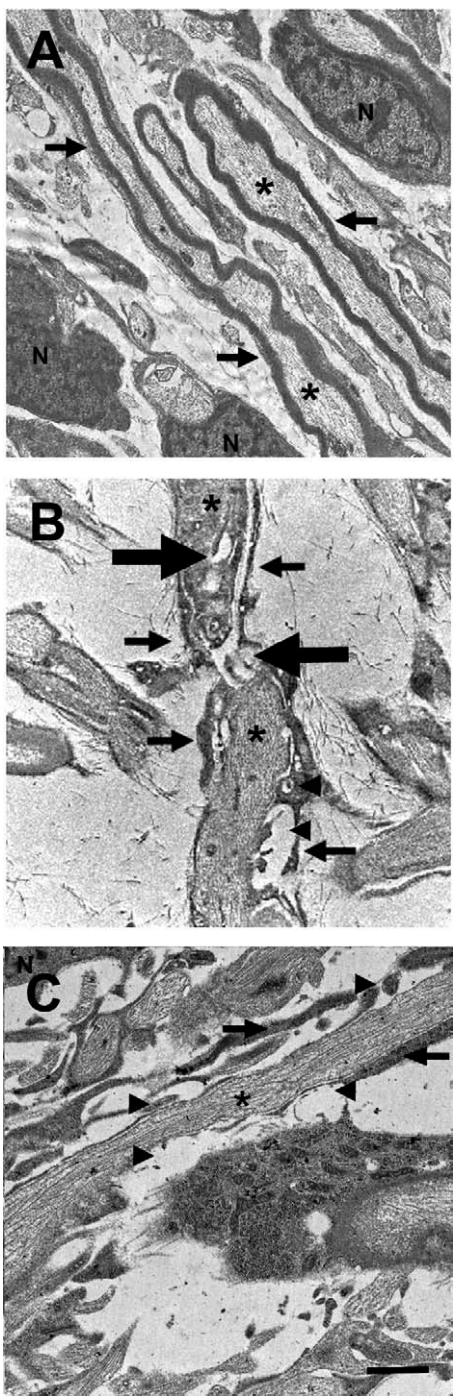

FIGURE 4: Biophysical stimuli induced demyelination without disruption of axonal ultrastructure. (A) A representative transmission electron microscopy image of control myelinating cocultures. Normal compact myelin (*arrows*) is seen uniformly and tightly wrapped around the internode of each axon (labeled with *asterisks*). Three Schwann cell nuclei (N) are visible. (B) A representative transmission electron microscope image of myelinating cocultures exposed to dichloroacetate (DCA) as a positive control. DCA-induced demyelination is associated with disruption of axonal ultrastructure (*large arrows*). Note the disruption of compact myelin (*small arrows*) and vacuole formation within the compact myelin (*arrowheads*). Also note that myelin is no longer tightly apposed to the axon (labeled with *asterisks*). (C) Biophysical stimuli-induced demyelination occurred without disruption of axonal ultrastructure. Shown is a representative image of myelinating coculture subjected to 24 hours of compression and hypoxia. The uniform, compact myelin structure (*arrows*) has been disrupted with segmentation, unraveling, and vacuole formation (*arrowheads*). Note that normal axonal ultrastructure is maintained (labeled with *asterisk*). One Schwann cell nuclei (N) is visible. Scale bar = 5μm.

Hydrostatic Compression Induces SC Proliferation

Interestingly, hydrostatic pressure stimulated SC proliferation, indicating possible phenotypic switch.[23] This phenomenon is similar to our in vivo observation that SCs increase in number within the first 4 weeks of CNC injury.[24] Following 24 hours of hydrostatic compression, there was a 2.6-fold increase in BrdU-labeled SCs compared to control (Fig 5C; control, 1.89 $\pm$ 0.54%, n = 16; compression, 4.93 $\pm$ 1.28%, n = 14; $p = 0.041$).

Because a small amount of gas is allowed to escape from the compression chamber during hydrostatic compression, a possible confounding effect of the chamber experiment is an increase in the osmolarity of the culture medium secondary to evaporation. Therefore, BrdU analysis was repeated in the presence of supplemental albumin to simulate increased osmolarity. The result indicates no increased apoptosis with increased osmolarity (see Fig 5C; high serum, 0.41 $\pm$ 0.15%, n = 4).

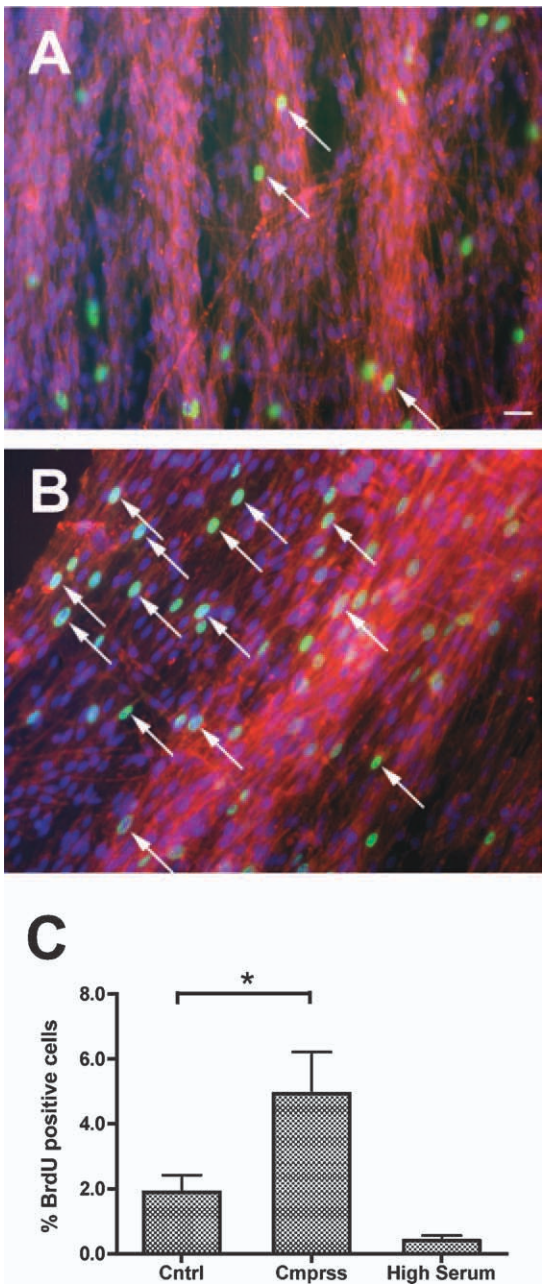

FIGURE 5: Hydrostatic compression induced proliferation of Schwann cells. Myelinated neuron–Schwann cell cocultures were compressed for 24 hours, and subsequently exposed to the nucleotide analogue 5′-bromo-2′-deoxyuridine (BrdU) for 1.5 hours. Cultures were then triple-immunostained for S100 (red), BrdU (green), and Schwann cell nuclei (blue). (A) An example image of control coculture shows the baseline amount of BrdU incorporation into Schwann cell nuclei. Scale bar = 50μm. (B) An example image of compressed coculture reveals a markedly increased number of BrdU-positive Schwann cell nuclei compared to control cocultures. (C) Summary plot showing percentage BrdU-positive nuclei in control cultures (Cntrl; left column), compressed cultures (Cmprss; middle column), and cultures exposed to high osmolarity (right column); asterisk indicates significant difference (*t* test, 1-tailed, $p = 0.041$).

In Vitro Injury Alters Phosphorylation of Integrin-Associated Signaling and Scaffolding Proteins

Biophysical Stimulation produces SC proliferation and demyelination, but what molecular pathways mediate this effect? Given the known role of the integrin signaling cascade in mediating cell–cell interactions, we explored whether hydrostatic compression and hypoxia would alter the phosphorylation state of different components of the integrin signaling pathway. Myelinated cocultures were exposed to hydrostatic pressure and hypoxia for varied durations, and Western blot analysis was used to assess the phosphorylation states of nonreceptor tyrosine kinase Src, focal adhesion kinase (FAK), the proline-rich tyrosine kinase 2 (Pyk2), as well as paxillin (Pax), a docking and actin cross-linking protein. Biophysical stimulation increased levels of Src phosphorylated at tyrosine 418, with levels rising with increasing duration of the biophysical stimulus up to 60 minutes (Fig 6A, blue curve). No significant differences in the phosphorylation state of FAK, Pyk2, and Pax were detected (see Fig 6C; n = 3 each).

To test if the observed increase in Src phosphorylation is the result of integrin signaling, we treated cultures with integrin function-blocking antisera[25,26] during the application of biophysical stimuli. Because the great majority of known integrin dimers include an αV or β1 subunit, and because myelin is known to also express functionally important levels of the α6/β4 dimer,[10,27] we treated cocultures with a cocktail of antisera that block the function of the αV, β1, and β4 integrin subunits. By including all 3 function-blocking antibodies, integrin signaling of at least 15 dimers is abolished, as inactivation of 1 integrin subunit is known to inactivate the entire integrin dimer (illustrated in Fig 6E). Application of the function blocking antisera cocktail completely abolished the increases in phospho-Src otherwise induced by hydrostatic compression and hypoxia (see Fig 6A, green curve).

Functional Blockade of Integrin Signaling Alleviates Stimulation-Induced Demyelination

Having observed that functional blockade of integrin signaling abrogated the increased phosphorylation of pSrc in response to biophysical stimuli, we asked whether abolishing integrin signaling would also block biophysical stimuli-induced demyelination. Myelinated cocultures were subjected to 24 hours of hydrostatic compression and hypoxia in the presence of the integrin-neutralizing antisera cocktail. Quantification of demyelination via MBP staining consistently indicated a significant diminution of pressure-induced demyelination in cultures

treated with the antibody cocktail (Fig 7C). Stimulation of cocultures in normal medium resulted in 2.4% demyelination. After the introduction of function-blocking antibodies in the culture medium, the observed demyelination decreased to 1.5% (n = 5; *t* test, $p = 0.042$, Fig 7D). Thus, although the antibody cocktail completely abolished Src phosphorylation and did markedly decrease biophysical stimuli-induced demyelination, it did not completely block this phenomenon.

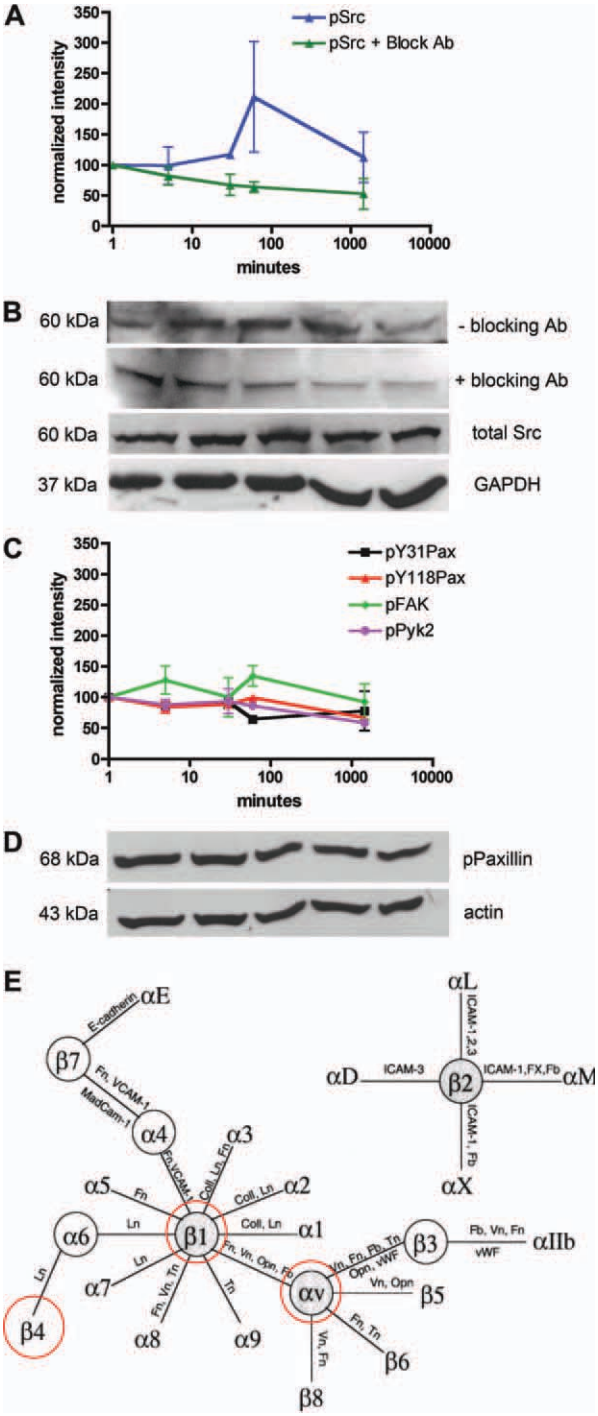

Biophysical Stimulation and Functional Blockade of Integrin Signaling Does Not Induce SC Degeneration as Determined by Oct-6 Expression

Prior to myelination, immature SCs transition from a promyelinating state into a myelinating state, a process requiring the precise coordination of several transcriptional factors. Oct-6 is a key SC transcription factor found to have particular importance in cultured SCs because it is involved in the regulation of the expression of the *Krox20/Egr2* gene, the product of which plays a key role in the maintenance of myelin in the peripheral nervous system. Upregulation of Oct-6 results in increased expression of myelination-associated genes,

FIGURE 6: Src phosphorylation increased transiently with biophysical stimuli via an integrin-dependent mechanism. For each experiment, 5 to 6 coculture coverslips were subjected to the indicated duration of hydrostatic compression and hypoxia and immediately removed from the bioreactor and placed into an ice-cooled culture plate. The cocultures were extracted using sodium dodecyl sulfate (SDS) lysis buffer (1% SDS, 50mM Tris, pH 8.0) containing phosphatase inhibitor cocktail (PhosSTOP; Roche Applied Science). Lysates of cocultures (50–75μg/lane) were separated on Western blot and probed with polyclonal antibodies (Abs) to phosphorylated versions of integrin-associated signaling molecules Src, Pax, FAK, and Pyk2. (A) Biophysical stimuli of myelinated cocultures increased phosphorylation of Src. In normal culture medium, phosphorylation at tyrosine 418 of Src was upregulated with increasing duration of compression and hypoxia up to 60 minutes but subsequently decreased to baseline (*blue solid line*). To verify that the observed signaling response was integrin mediated, the experiment was repeated in a cocktail of function-blocking integrin antibodies to determine the effect of silencing integrin signaling. In the presence of function-blocking integrin antibodies, the upregulation of Src phosphorylation was abolished (*green dotted line*; n = 3 at each time point). (B) Representative Western blots of coculture lysates probed with antibody recognizing pSrc (60kDa); biophysical stimuli were applied with the cocultures in normal (− blocking Ab) and in media containing function-blocking anti-integrin antibodies (+ blocking Ab); a representative blot was subsequently stripped and reprobed for total Src; the blots were also reprobed with anti–glyceraldehyde-3-phosphate dehydrogenase (GAPDH) antibodies (37kDa) as a protein loading control (GAPDH). (C) Biophysical stimuli had minimal effect on tyrosine phosphorylation of Pax, FAK, and Pyk2 (n = 3) each. (D) Representative Western blots of coculture lysates probed with an antibody recognizing phosphopaxillin at tyrosine 31 (68kDa) show no significant change in the extent of tyrosine phosphorylation in response to biophysical stimulation; the blot was reprobed with actin (43kDa) as loading control. (E) A schematic diagram shows known integrin dimer combinations; because the blockade of 1 subunit leads to inactivation of the integrin dimer, functional blockade of αV, β1, and β4 (*red circles*) leads to inactivation of 15 integrin dimer combinations; modified from Milner and Campbell (2002).[27] [Color figure can be viewed in the online issue, which is available at www.annalsofneurology.org.]

whereas deletion of Oct-6 leads to a delay in the switch to the myelinating phenotype.[28]

Having characterized the biophysical stimuli involved in demyelination, we wondered whether the observed demyelination in our cocultures system is associated with changes in Oct-6 expression. Myelinating neuronal-SC cocultures were subjected to 24 hours of hydrostatic pressure and hypoxia in normal medium or in medium containing function-blocking integrin antibodies. Immunohistochemistry and confocal images were then obtained to determine differential expression of Oct-6. There was no detectable change in Oct-6 expression in response to hydrostatic compression or to integrin silencing (see Fig 7E–G).

Nonreceptor Tyrosine Kinase Src Colocalizes with SCs

Given the data above implicating Src phosphorylation as a critical initiating step, it was of significant interest to determine whether the hydrostatic compression-induced upregulation of Src phosphorylation occurred in SCs. Cocultures that had been stimulated for 60 minutes were triply immunostained with antisera to phospho-Src (Tyr 418), the pan SC marker S100, and axonal marker neurofilament (Fig 8). Colocalization analyses were then performed using IMARIS software to determine whether the pSrc signals colocalized with S100 or neurofilament signals. Colocalization analysis yielded colocalization coefficient of 59.94 for pSrc with S100, and 25.79 for pSrc with neurofilament. Surface reconstructions of high-resolution confocal images revealed the presence of pSrc in SCs (see Fig 8C). Taken together, these results indicate that the activated secondary messengers are located within SCs, implicating SCs as a mediator of the observed injury response.

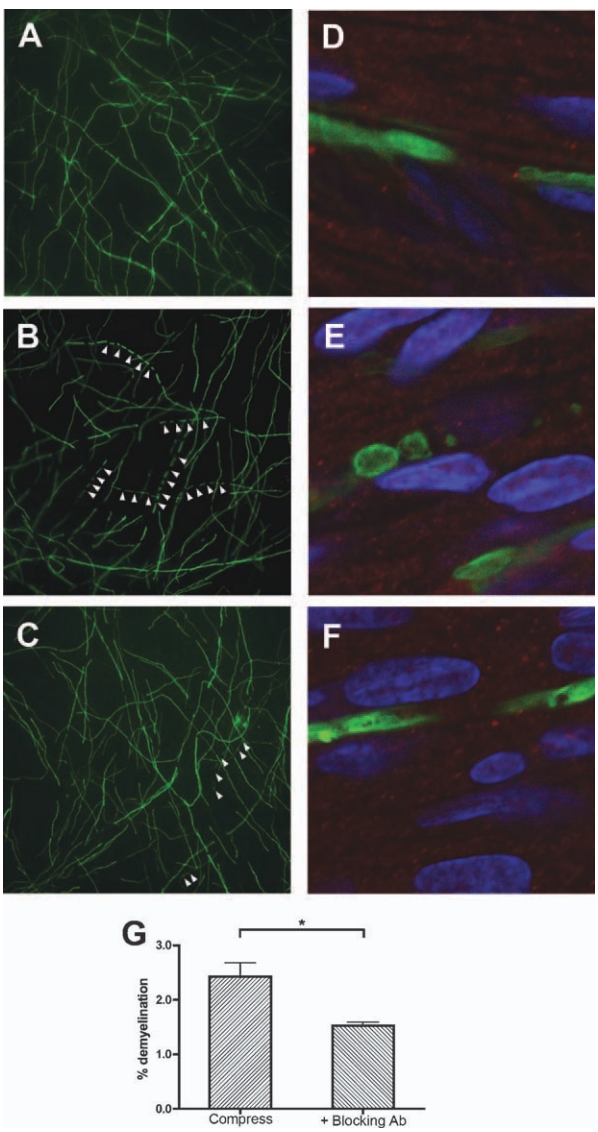

FIGURE 7: Functional blockade of integrin signaling alleviated hydrostatic pressure-induced demyelination. Myelinating neuron–Schwann cell cocultures were subjected to 24 hours of hydrostatic pressure and hypoxia without (− Blocking Ab) and with (+ Blocking Ab) function-blocking integrin antibodies (n = 5). Subsequent to stimulation, coculture coverslips were assessed for demyelination (see Materials and Methods). Representative fluorescent images of coverslips are shown for comparison. (A) A noncompressed sample is shown for baseline comparison. (B) Samples subjected to 24 hours of hydrostatic compression and hypoxia are shown. Six axons are seen with fragmented myelin (*arrowheads*). (C) Samples stimulated in the presence of integrin function-blocking antibodies had identical appearance but significantly less demyelination. Three axons are seen with fragmented myelin and myelin ovoids (*arrowheads*). (D) Blocking integrin signaling alleviated stimulation-induced demyelination by an average of 47%. Although 1 trial was not quite statistically significant (p = 0.058, *t* test, 1-tailed), repeated experiment yielded a statistically significant difference in mean value between the control and blockade groups (*p = 0.042, *t* test, 1-tailed); error bars represent standard error of the mean. To determine whether Schwann cells undergo degeneration in response to hydrostatic compression, we assessed Oct-6 expression in control samples (E), compressed samples (F), and in samples compressed in the presence of function-blocking integrin antibodies (G). Analysis with high-power confocal microscopy showed no difference in the pattern or intensity of Oct-6 staining regardless of treatment.

Discussion

Direct mechanical stimulation is known to modulate cellular activity in a variety of biological systems including bone, cartilage, and the vascular system.[29–32] Mechanical stimuli are potent mitogens for mechanosensitive cells such as fibroblasts and osteoblasts.[33,34] Increasing evidence suggests that neural tissues are also directly mechanically sensitive. For example, SCs respond to fluid shear stress in part by proliferating and downregulating myelin-associated genes.[6] We show here that applied hydrostatic pressure triggers SC proliferation and

demyelination in a way that is similar to what occurs in vivo despite the maintenance of normal oxygen tension, pH, and available nutrients. These findings provide further evidence that neural tissues can respond directly to pressure. Moreover, because only 2 cell types exist in the cocultures, mechanosensitivity must exist within the neurons, the SCs, or possibly the interface between them.

We observed demyelination without detectable changes in axonal structure when investigated under high-resolution confocal microscopy or electron microscopy. Similarly, there was no detectable cell lysis or apoptosis as assayed by LDH release and TUNEL analysis in response to hydrostatic compression, hypoxia, or glucose deprivation applied individually or in combinations that induced demyelination. Taken together, these results suggest that biophysical stimuli cause demyelination independent of neuronal or SC death. In contrast to our observations, a recent study showed that pure DRG cultures exhibit cell death in response to mechanical stimuli and hypoxia.[35] However, with those experiments, neuronal cultures were exposed to supraphysiologic loading conditions of an alternative mechanical stimulus (ie, 20% tensile strain).

We demonstrate that demyelination is more severe when hydrostatic compression occurs under conditions of hypoxia, a result suggesting that cellular metabolism plays an important role in the maintenance of myelin structure. Myelin formation entails high metabolic demand due to the need for SCs to synthesize large quantities of myelin-related lipids and proteins. Although little is known about the energy requirements of mature myelin, its highly specialized membrane domains may render it sensitive to metabolic insults.[36] Experimental studies using a rat model of focal glucose deprivation showed that cerebral white matter is highly vulnerable to metabolic disruption, with oligodendrocyte death preceding the appearance of necrotic neurons.[37] Similarly, exposure of rats to elemental tellurium, which inhibits the biosynthesis of cholesterol, results in reversible demyelination due to a preferential affect on myelinating SCs.[38] Furthermore, the glycolysis inhibitor dichloroacetate also induces reversible demyelination in neuron/SC cocultures.[22] Together, these results suggest that altering the delicate metabolic balance of SCs may predispose myelin to destabilization. This stringent metabolic requirement may explain why diabetes, which

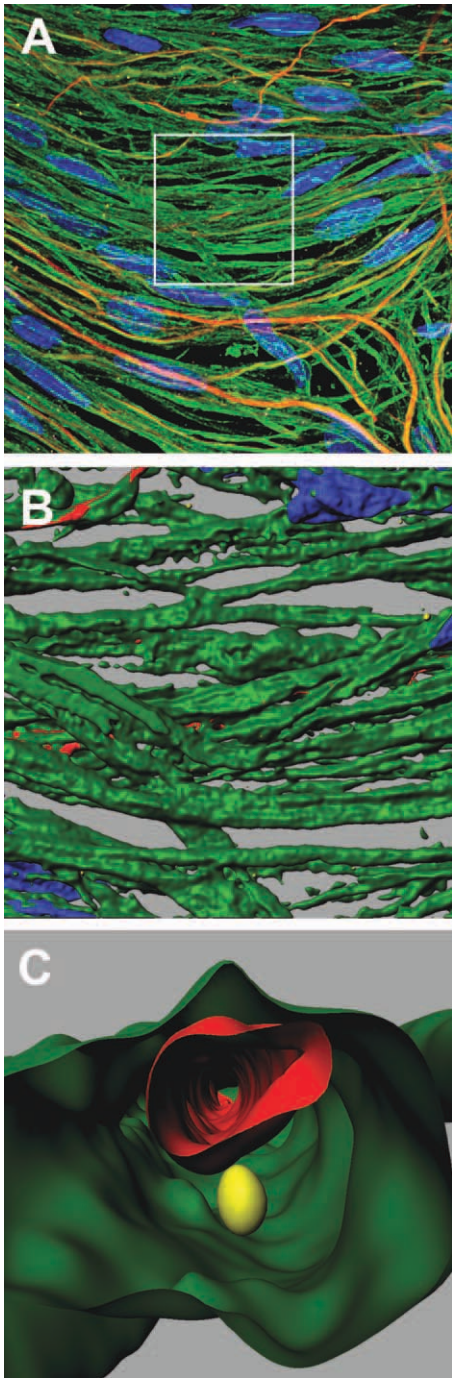

FIGURE 8: The nonreceptor tyrosine kinase Src colocalized with Schwann cells. Myelinated cocultures were subjected to hydrostatic compression and hypoxia for 60 minutes and triple-immunolabeled for S100, neurofilament, and pSrc. High-resolution confocal images were taken to determine whether pSrc colocalizes with Schwann cells or with neurons. (A) Transparent composite 3-dimensional (3D) Z-stack shows all 3 signals. S100 signal (green) shows the filamentous arrangement of Schwann cell cytoplasm wrapping around neurofilament signals (red). pSrc signals (yellow) are punctate, possibly reflecting the location of focal adhesions. The Schwann cell nuclei are DAPI labeled and are shown in blue. (B) Opaque 3D volumetric surface rendering overlay of inset in panel A is shown. Most of colocalized neurofilament and pSrc is now masked because it is located within the opaque reconstructed S100 surface. (C) Zoomed-in perspective shows an example of pSrc localization within a rendered 3D volumetric surface using IMARIS 3D visualization. Colocalized pSrc signals (yellow) are within the rendered Schwann cell surface (green) and outside of the rendered neurofilament surface (red).

predisposes patients to vasculopathy, also increases a patient's susceptibility to developing CNC injuries.

Our findings are in keeping with other evidence that integrins are capable of acting as mechanoreceptors in mechanosensitive cells such as fibroblasts, osteoblasts, and chondrocytes. Hydrostatic pressure is a unique form of mechanical stimulation in that it has little affect on cellular morphology and volume, yet physiologic levels of hydrostatic pressures have been noted to alter cellular activity[39–41] and cytoskeleton polymerization.[42,43]

SCs are known to play critical roles in regulating the maturation, maintenance, and viability of axons.[44,45] Compelling evidence now indicates that SCs play pivotal roles in the pathogenesis of CNC injury, as the CNC-induced SC proliferative response precedes the characteristic demyelination and remyelination response.[24,46] Mechanical loading of SCs alters the expression of genes that permit axonal sprouting, a response observed in later stages of chronic compression injury.[6,47] Our results reported here, colocalizing SCs with the messenger protein Src activated in response to demyelinating biophysical stimuli, further implicate SCs as the prime mediator of CNC injury.

Here we show, using a novel in vitro model, that hydrostatic compression of neuronal tissue directly triggers demyelination and SC proliferation. This injury response is associated with the activation of Src phosphorylation in SCs; blocking this response abrogates cellular responses to compression injury. We show that hypoxia and glucose deprivation, the secondary effects attributable to compression-induced disruption of peripheral nerve microcirculation, potentiate the injury response but in isolation have little effect on myelin integrity. Our results implicate the integrin pathway as a key mediator of the cellular changes underlying compression neuropathy, and point to SCs as the key player mediating the pathogenesis of CNC injury.

Acknowledgments

This work was supported by NIH National Institute of Neurological Disorders and Stroke grant 2R01NS049203-06A1 (Ranjan Gupta) and National Institutes of Mental Health grant MH082042 (Christine Gall).

Potential Conflicts of Interest

Nothing to report.

References

1. Mizisin AP, Kalichman MW, Myers RR, Powell HC. Role of the blood-nerve barrier in experimental nerve edema. Toxicol Pathol 1990;18:170–185.
2. Lundborg G, Dahlin LB. Anatomy, function, and pathophysiology of peripheral nerves and nerve compression. Hand Clin 1996;12:185–193.
3. Ko C, Brown TD. A fluid-immersed multi-body contact finite element formulation for median nerve stress in the carpal tunnel. Comput Methods Biomech Biomed Engin 2007;10:343–349.
4. Blackman BR, Barbee KA, Thibault LE. In vitro cell shearing device to investigate the dynamic response of cells in a controlled hydrodynamic environment. Ann Biomed Eng 2000;28:363–372.
5. Halka AT, Turner NJ, Carter A, et al. The effects of stretch on vascular smooth muscle cell phenotype in vitro. Cardiovasc Pathol 2008;17:98–102.
6. Gupta R, Truong L, Bear D, et al. Shear stress alters the expression of myelin-associated glycoprotein (MAG) and myelin basic protein (MBP) in Schwann cells. J Orthop Res 2005;23:1232–1239.
7. Sahara M, Sata M, Matsuzaki Y, et al. Comparison of various bone marrow fractions in the ability to participate in vascular remodeling after mechanical injury. Stem Cells 2005;23:874–878.
8. Reilly GC, Haut TR, Yellowley CE, et al. Fluid flow induced PGE2 release by bone cells is reduced by glycocalyx degradation whereas calcium signals are not. Biorheology 2003;40:591–603.
9. Hynes RO. Integrins: versatility, modulation, and signaling in cell adhesion. Cell 1992;69:11–25.
10. Previtali SC, Feltri ML, Archelos JJ, et al. Role of integrins in the peripheral nervous system. Prog Neurobiol 2001;64:35–49.
11. Aplin AE, Howe A, Alahari SK, Juliano RL. Signal transduction and signal modulation by cell adhesion receptors: the role of integrins, cadherins, immunoglobulin-cell adhesion molecules, and selectins. Pharmacol Rev 1998;50:197–263.
12. Hynes RO. Integrins: bidirectional, allosteric signaling machines. Cell 2002;110:673–687.
13. Giancotti FG, Tarone G. Positional control of cell fate through joint integrin/receptor protein kinase signaling. Annu Rev Cell Dev Biol 2003;19:173–206.
14. Banker G, Goslin K. Culturing nerve cells. 2nd ed. Cambridge, MA: MIT Press, 1998.
15. Brockes JP, Raff MC. Studies on cultured rat Schwann cells. II. Comparison with a rat Schwann cell line. In Vitro 1979;15:772–778.
16. Frieboes LR, Gupta R. An in-vitro traumatic model to evaluate the response of myelinated cultures to sustained hydrostatic compression injury. J Neurotrauma 2009;26:2245–2256.
17. Larsen JO. Stereology of nerve cross sections. J Neurosci Methods 1998;85:107–118.
18. Costes SV, Daelemans D, Cho EH, et al. Automatic and quantitative measurement of protein-protein colocalization in live cells. Biophys J 2004;86:3993–4003.
19. Levy H, Assaf Y, Frenkel D. Characterization of brain lesions in a mouse model of progressive multiple sclerosis. Exp Neurol 2010;226:148–158.
20. Brace H, Latimer M, Winn P. Neurotoxicity, blood-brain barrier breakdown, demyelination and remyelination associated with NMDA-induced lesions of the rat lateral hypothalamus. Brain Res Bull 1997;43:447–455.
21. Arroyo EJ, Sirkowski EE, Chitale R, Scherer SS. Acute demyelination disrupts the molecular organization of peripheral nervous system nodes. J Comp Neurol 2004;479:424–434.
22. Felitsyn N, Stacpoole PW, Notterpek L. Dichloroacetate causes reversible demyelination in vitro: potential mechanism for its neuropathic effect. J Neurochem 2007;100:429–436.
23. Chao T, Pham K, Steward O, Gupta R. Chronic nerve compression injury induces a phenotypic switch of neurons within the dorsal root ganglia. J Comp Neurol 2008;506:180–193.

24. Gupta R, Steward O. Chronic nerve compression induces concurrent apoptosis and proliferation of Schwann cells. J Comp Neurol 2003;461:174–186.
25. Lin CY, Hilgenberg LG, Smith MA, et al. Integrin regulation of cytoplasmic calcium in excitatory neurons depends upon glutamate receptors and release from intracellular stores. Mol Cell Neurosci 2008;37:770–780.
26. Bernard-Trifilo JA, Kramar EA, Torp R, et al. Integrin signaling cascades are operational in adult hippocampal synapses and modulate NMDA receptor physiology. J Neurochem 2005;93:834–849.
27. Milner R, Campbell IL. The integrin family of cell adhesion molecules has multiple functions within the CNS. J Neurosci Res 2002; 69:286–291.
28. Svaren J, Meijer D. The molecular machinery of myelin gene transcription in Schwann cells. Glia 2008;56:1541–1551.
29. Yu W, Khandelwal P, Apodaca G. Distinct apical and basolateral membrane requirements for stretch-induced membrane traffic at the apical surface of bladder umbrella cells. Mol Biol Cell 2009; 20:282–295.
30. Pavalko FM, Norvell SM, Burr DB, et al. A model for mechanotransduction in bone cells: the load-bearing mechanosomes. J Cell Biochem 2003;88:104–112.
31. Mizuno S. A novel method for assessing effects of hydrostatic fluid pressure on intracellular calcium: a study with bovine articular chondrocytes. Am J Physiol Cell Physiol 2005;288:C329–C337.
32. Muller S, Labrador V, Da Isla N, et al. From hemorheology to vascular mechanobiology: an overview. Clin Hemorheol Microcirc 2004;30:185–200.
33. Carracedo S, Lu N, Popova SN, et al. The fibroblast integrin alpha11beta1 is induced in a mechanosensitive manner involving activin A and regulates myofibroblast differentiation. J Biol Chem 2010;285:10434–10445.
34. Malone AM, Anderson CT, Tummala P, et al. Primary cilia mediate mechanosensing in bone cells by a calcium-independent mechanism. Proc Natl Acad Sci U S A 2007;104:13325–13330.
35. Gladman SJ, Ward RE, Michael-Titus AT, et al. The effect of mechanical strain or hypoxia on cell death in subpopulations of rat dorsal root ganglion neurons in vitro. Neuroscience 2010;171: 577–587.
36. Morell P, Toews AD. Schwann cells as targets for neurotoxicants. Neurotoxicology 1996;17:685–695.
37. Pantoni L, Garcia JH, Gutierrez JA. Cerebral white matter is highly vulnerable to ischemia. Stroke 1996;27:1641–1646; discussion 1647.
38. Toews AD, Hostettler J, Barrett C, Morell P. Alterations in gene expression associated with primary demyelination and remyelination in the peripheral nervous system. Neurochem Res 1997;22: 1271–1280.
39. Tarnok A, Ulrich H. Characterization of pressure-induced calcium response in neuronal cell lines. Cytometry 2001;43:175–181.
40. Lammi MJ, Elo MA, Sironen RK, et al. Hydrostatic pressure-induced changes in cellular protein synthesis. Biorheology 2004; 41:309–313.
41. Smith RL, Carter DR, Schurman DJ. Pressure and shear differentially alter human articular chondrocyte metabolism: a review. Clin Orthop Relat Res 2004;(427 suppl):S89–S95.
42. Myers KA, Rattner JB, Shrive NG, Hart DA. Hydrostatic pressure sensation in cells: integration into the tensegrity model. Biochem Cell Biol 2007;85:543–551.
43. Knight MM, Toyoda T, Lee DA, Bader DL. Mechanical compression and hydrostatic pressure induce reversible changes in actin cytoskeletal organisation in chondrocytes in agarose. J Biomech 2006;39:1547–1551.
44. Court FA, Hendriks WT, Macgillavry HD, et al. Schwann cell to axon transfer of ribosomes: toward a novel understanding of the role of glia in the nervous system. J Neurosci 2008;28: 11024–11029.
45. Riethmacher D, Sonnenberg-Riethmacher E, Brinkmann V, et al. Severe neuropathies in mice with targeted mutations in the ErbB3 receptor. Nature 1997;389:725–730.
46. Gupta R, Rowshan K, Chao T, et al. Chronic nerve compression induces local demyelination and remyelination in a rat model of carpal tunnel syndrome. Exp Neurol 2004;187:500–508.
47. Gupta R, Rummler LS, Palispis W, et al. Local down-regulation of myelin-associated glycoprotein permits axonal sprouting with chronic nerve compression injury. Exp Neurol 2006;200: 418–429.